

Article

Oligoorganogermanes: Interplay between Aryl and Trimethylsilyl Substituents

Kirill V. Zaitsev ^{1,2,*} , Oleg Kh. Poleshchuk ^{3,4} and Andrei V. Churakov ⁵ 

¹ Department of Chemistry, M.V. Lomonosov Moscow State University, Leninskie Gory 1, 3, 119991 Moscow, Russia

² A.V. Topchiev Institute of Petrochemical Synthesis, Russian Academy of Sciences, Leninskii Prospekt 29, 119991 Moscow, Russia

³ Faculty of Chemistry, National Research Tomsk State University, Lenin Avenue 36, 634050 Tomsk, Russia; poleshch@tspu.edu.ru

⁴ Department of Chemistry, Tomsk State Pedagogical University, Kievskaya Street 60, 634061 Tomsk, Russia

⁵ N.S. Kurnakov Institute of General and Inorganic Chemistry, Russian Academy of Sciences, Leninskii Prospekt 31, 117901 Moscow, Russia; churakov@igic.ras.ru

* Correspondence: zaitsev@org.chem.msu.ru; Tel.: +7-495-939-3887

Abstract: Derivatives of main group elements containing element–element bonds are characterized by unique properties due to σ -conjugation, which is an attractive subject for investigation. A novel series of digermanes, $\text{Ar}_3\text{Ge-Ge}(\text{SiMe}_3)_3$, containing aryl ($\text{Ar} = p\text{-C}_6\text{H}_4\text{Me}$ (**1**), $p\text{-C}_6\text{H}_4\text{F}$ (**2**), C_6F_5 (**3**)) and trimethylsilyl substituents, was synthesized by the reaction of germyl potassium salt, $[(\text{Me}_3\text{Si})_3\text{GeK}^*\text{THF}]$, with triarylchlorogermanes, Ar_3GeCl . The optical and electronic properties of such substituted oligoorganogermanes were investigated spectroscopically by UV/vis absorption spectroscopy and theoretically by DFT calculations. The molecular structures of compounds **1** and **2** were studied by XRD analysis. Conjugation between all structural fragments (Ge-Ge , Ge-Si , Ge-Ar , where Ar is an electron-donating or withdrawing group) was found to affect the properties.

Keywords: organogermanium compounds; oligoorganogermanes; donor–acceptor molecules; element–element bond; group 14 elements; σ -conjugation; single-crystal XRD analysis; UV/vis absorption; DFT calculations; main group metal chemistry



Citation: Zaitsev, K.V.; Poleshchuk, O.K.; Churakov, A.V. Oligoorganogermanes: Interplay between Aryl and Trimethylsilyl Substituents. *Molecules* **2022**, *27*, 2147. <https://doi.org/10.3390/molecules27072147>

Academic Editor: Franck Camerel

Received: 17 February 2022

Accepted: 24 March 2022

Published: 26 March 2022

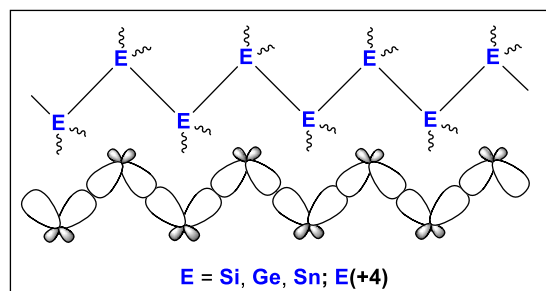
Publisher's Note: MDPI stays neutral with regard to jurisdictional claims in published maps and institutional affiliations.



Copyright: © 2022 by the authors. Licensee MDPI, Basel, Switzerland. This article is an open access article distributed under the terms and conditions of the Creative Commons Attribution (CC BY) license (<https://creativecommons.org/licenses/by/4.0/>).

1. Introduction

Research into organic derivatives of main group elements is a topical issue of organometallic chemistry [1–4]. Many efforts have been made to develop improved synthetic methods, determine new properties, find relationships between structures and properties, and produce novel materials. Some of the main group element derivatives are molecular compounds of group 14 elements ($\text{E} = \text{Si}$ [5], Ge [6], Sn [7], Pb [8]) [9] containing element–element bonds (oligoorganotetrelanes). Unusual properties (UV/vis absorbance, luminescence, electrochemical activity, thermochromism, etc.) that appear in these compounds due to σ -conjugation [10] (Scheme 1) are of evident research interest [11].



Scheme 1. Schematic representation of oligoorganotetrelanes.

Compounds **1–3** were isolated as white powders with high solubility in all typical organic solvents including *n*-hexane, indicating their weak polarity and emphasizing yet again their analogy to alkanes. The compounds were characterized by NMR (^1H , ^{13}C , ^{19}F) (Supplementary Materials, Figures S1–S11) and UV/visible (Supplementary Materials, Figures S12–S14) spectroscopy, elemental analysis and X-ray diffraction analysis.

2.2. NMR Spectroscopy

The main NMR spectral parameters for compounds **1–3** (CDCl_3 , RT) are quite similar; the presence of one set of signals for each compound is characteristic of molecules with a highly symmetric structure (C_{3v} symmetry) in solution with free rotation of different molecular fragments.

2.3. XRD Structures

The molecular structures of molecular oligoorganogermanes **1** and **2** were studied in a crystal by X-ray diffraction analysis (Figures 1 and 2; Supplementary Materials, Table S1). Interestingly, the molecular structures of compounds with the $\text{Si}_3\text{Ge-GeC}_3$ framework have not been studied previously.

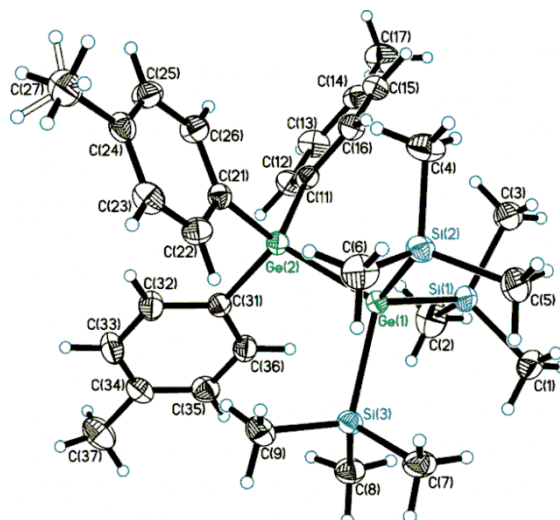


Figure 1. Molecular structure of compound $(\text{Me}_3\text{Si})_3\text{Ge-Ge}(\text{C}_6\text{H}_4\text{Me-}p)_3$ (**1**). Displacement ellipsoids are shown at a 50% probability level. Minor component of disordered Me group is drawn by open lines. Selected bond lengths (Å) and bond angles (deg): Ge(1)–Ge(2) 2.4393(2), Ge(1)–Si_{av} 2.3864(4), Ge(2)–C_{av} 1.9601(14); Si–Ge(1)–Si_{av} 107.973(16), Si–Ge(1)–Ge(2)_{av} 110.931(12), C–Ge(2)–C_{av} 107.68(6), C–Ge(2)–Ge(1)_{av} 111.21(4).

The structural parameters of **1** and **2** are similar; an insignificant elongation of bond lengths is observed only at transition to **2**, containing electron-withdrawing substituents. This structural feature has been observed in such donor–acceptor oligoorganogermanes earlier [21]. The key Ge–Ge bond length is typical of digermanes (2.4393(2), 2.4431(3) Å vs. 2.393(3) [Ph₂(O₂CCl₃)Ge–Ge(O₂CCl₃)Ph₂] [32]–2.4787(7) [(Me₃Si)₃Ge–Ge(SiMe₃)₃] [22] Å; cf. 2.419(1) Å in (*p*-MeC₆H₄)₃Ge–Ge(C₆H₄Me-*p*)₃ [33] and 2.4209(8) Å in (*p*-FC₆H₄)₃Ge–Ge(C₆H₄F-*p*)₃ [34]), and the presence of sterically bulk hypergermyl, Hge [35,36], Ge(SiMe₃)₃ groups affects the elongation of the bond parameters. The Ge–Si bond lengths (average values, 2.3864(4) and 2.3908(5) Å, respectively) are within the normal range of 2.38–2.41 Å [22,37].

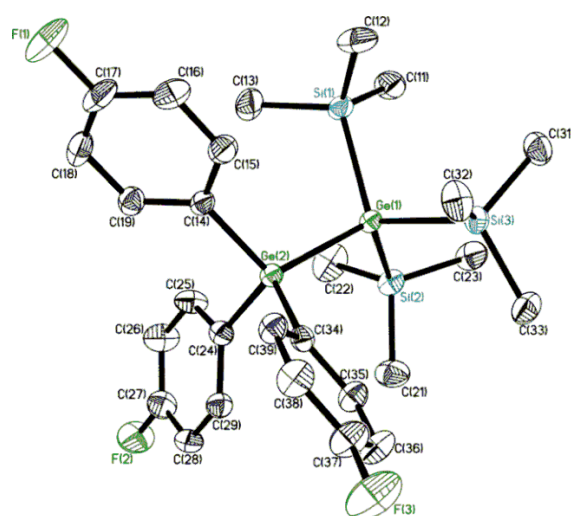


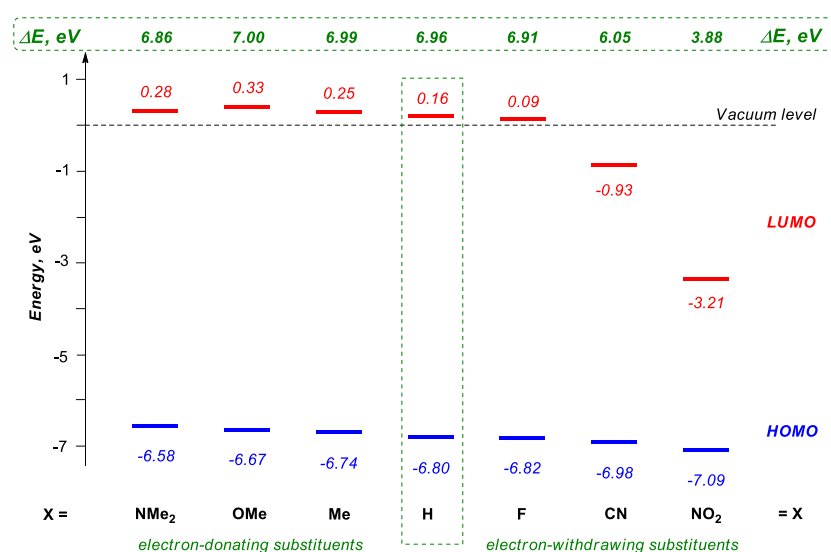
Figure 2. Molecular structure of compound $(\text{Me}_3\text{Si})_3\text{Ge}-\text{Ge}(\text{C}_6\text{H}_4\text{F}-p)_3$ (**2**). Only one independent molecule is drawn. Displacement ellipsoids are shown at a 50% probability level. Hydrogen atoms are omitted for clarity. Selected bond lengths (\AA) and bond angles (deg): $\text{Ge}(1)-\text{Ge}(2)$ 2.4431(3), $\text{Ge}(1)-\text{Si}_{\text{av}}$ 2.3908(5), $\text{Ge}(2)-\text{C}_{\text{av}}$ 1.9625(16); $\text{Si}-\text{Ge}(1)-\text{Si}_{\text{av}}$ 109.350(18), $\text{Si}-\text{Ge}(1)-\text{Ge}(2)_{\text{av}}$ 109.590(14), $\text{C}-\text{Ge}(2)-\text{C}_{\text{av}}$ 107.49(7), $\text{C}-\text{Ge}(2)-\text{Ge}(1)_{\text{av}}$ 111.39(5).

Germanium atoms in **1** and **2** adopt a slightly distorted tetrahedral geometry, T-4 (angle values vary within the range of 107° – 112°). Tetrahedral τ_4 parameters, $\tau_4 = (360^\circ - \alpha - \beta)/141^\circ$ (α , β are the largest bond angles) [38], are varied in the 0.96–0.99 range for Ge atoms in **1** and **2** ($\tau_4 = 1$ for an ideal T-4 geometry). The conformations of both molecules along the Ge-Ge bond (average Si-Ge-Ge-C torsions, $92.83(4)/27.17(4)^\circ$ and $100.61(5)/19.39(5)^\circ$, respectively) can be described as distorted staggered (*ortho*-, *O*-/*cisoid*-, *C*- in terms of West [39]), which is noticeably different from the evident ideal 60° case (C_{3v} symmetry). At the same time, in mixed $(\text{Me}_3\text{Si})_3\text{Ge}-\text{GeAr}_3$ the torsion distortion is more significant than in the parent compound $(\text{Me}_3\text{Si})_3\text{Ge}-\text{Ge}(\text{SiMe}_3)_3$ (average Si-Ge-Ge-Si torsions, $76.82/43.18^\circ$) or $(p\text{-FC}_6\text{H}_4)_3\text{Ge}-\text{Ge}(\text{C}_6\text{H}_4\text{F}-p)_3$ (average Si-Ge-Ge-C torsions, $60.7(8)^\circ$). Thus, we can conclude that the introduction of sterically voluminous groups (such as trimethylsilyl instead of aryl) into catenated germanes affects the conformations more substantially (cf. the electron inducing eclipsed conformation in donor–acceptor digermanes [21]). Such torsion changes can even be accompanied by Ge-Ge bond length elongation.

Interestingly, the crystal of oligoorganogermane **2** is isostructural to $\text{Ph}_3\text{Al}^*\text{As}(\text{SiMe}_3)_3$ [40], indicating a similarity between crystals of different main group elements (Ge vs. Al, As).

2.4. DFT Calculations

We performed DFT calculations to clarify the properties of investigated digermanes using model compounds, $(\text{Me}_3\text{Si})_3\text{Ge}-\text{Ge}(\text{C}_6\text{H}_4\text{X}-p)_3$, in which the electronic properties of the Ar group were changed. In addition to the parent compound $(\text{Me}_3\text{Si})_3\text{Ge}-\text{GePh}_3$ ($\text{X} = \text{H}$), we studied electron-donating ($\text{X} = \text{Me}$, OMe , NMe_2) and electron-withdrawing ($\text{X} = \text{F}$, CN , NO_2) substituents in the aromatic ring. The levels of the HOMO and LUMO (lowest unoccupied molecular orbital) as well as the frontier orbital energy gap (ΔE) are presented in Scheme 3.



Scheme 3. Schematic representation of HOMO, LUMO levels and HOMO/LUMO gap (ΔE) in model digermanes $(\text{Me}_3\text{Si})_3\text{Ge-Ge}(\text{C}_6\text{H}_4\text{X-}p)_3$.

It should be noted one more time that before this work only $(\text{Me}_3\text{Si})_3\text{Ge-GePh}_3$ ($X = \text{H}$) [27,41] had been synthesized and investigated.

We found that the change of the electron properties of the Ar group in $(\text{Me}_3\text{Si})_3\text{Ge-Ge}(\text{C}_6\text{H}_4\text{X-}p)_3$ determined the energy of frontier orbitals. At the introduction of electron donating groups, the HOMO level was destabilized (increased in energy); this has been observed earlier by Weinert et al. [20] for related derivatives. At the same time, the LUMO level was also destabilized, but the general change of the HOMO/LUMO gap was insignificant. The narrowing of the energy gap in $(\text{Me}_3\text{Si})_3\text{Ge-Ge}(\text{C}_6\text{H}_4\text{X-}p)_3$ was observed only for strong donors ($X = \text{NMe}_2$). A more complex situation was observed for electron-withdrawing groups; it depended strongly on the type of X. The typical feature in this case was the stabilization of the HOMO level; a stronger acceptor led to a greater energy decrease. Furthermore, a stronger acceptor led to a more significant LUMO stabilization, especially in comparison with the HOMO level change. In other words, in the case of electron-withdrawing substituents X, the decrease in the ΔE associated first of all with the stabilization of LUMO, leading to a remarkable decrease in its energy level. All this indicates that the introduction of strong withdrawing substituents should lead to a more significant HOMO/LUMO gap decrease. The most striking data were obtained for a yet unknown (calculated but not yet synthesized) NO_2 derivative, which challenges the need for such compounds.

The distribution of electron density in HOMO and LUMO orbitals in $(\text{Me}_3\text{Si})_3\text{Ge-Ge}(\text{C}_6\text{H}_4\text{F-}p)_3$ (**2**) is presented in Figure 3; the data for $(\text{Me}_3\text{Si})_3\text{Ge-GePh}_3$ are given in Supplementary Materials (Figure S14). For these digermanes, $(\text{Me}_3\text{Si})_3\text{Ge-GeAr}_3$, the HOMO was distributed on the Ge-Ge bond with the inclusion of an Ar group, but to a lesser extent, which is typical of aryl oligoorganogermanes. The more stabilized HOMO-1 and HOMO-2 are localized on Ge-Si bonds. As is typical of arylgermanes, the LUMO and the higher-energy LUMO+1 and LUMO+2 were concentrated on aryl substituents. These data indicate that UV/vis absorption (Table 1) corresponds to σ, π -transitions (Ge-Ge-Si to Ar), making the absorbance bands (see below), to some extent, less intensive in comparison with related compounds, where the HOMO and LUMO are on E-E bonds (σ -transitions, as in fully alkylated or alkylsilylated oligogermanes).

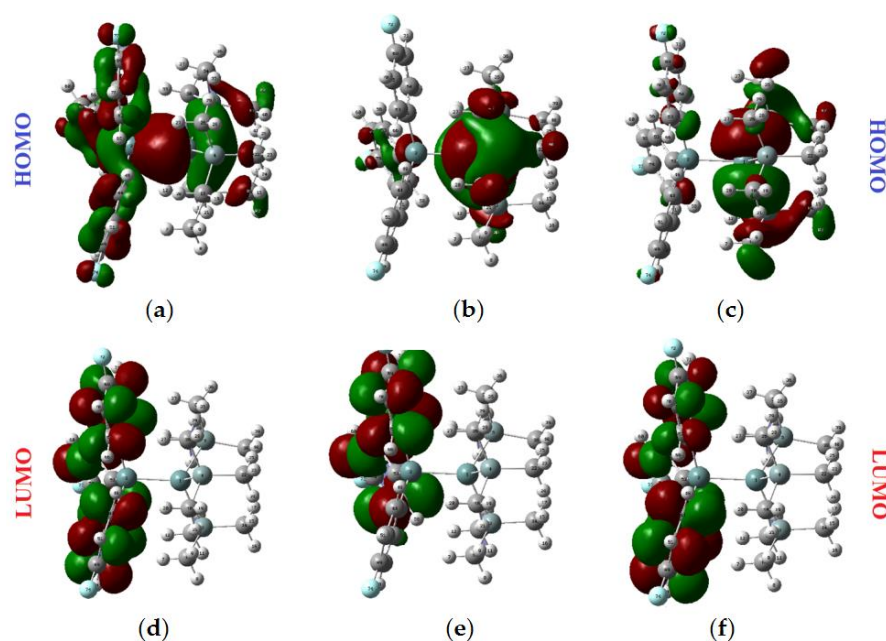


Figure 3. Graphical representation of the frontier orbitals of $(\text{Me}_3\text{Si})_3\text{Ge-Ge}(\text{C}_6\text{H}_4\text{F-}p)_3$ (2): (a) HOMO; (b) HOMO-1; (c) HOMO-2; (d) LUMO; (e) LUMO+1; (f) LUMO+2.

Table 1. Data of DFT calculations for compounds of the type of $(\text{Me}_3\text{Si})_3\text{Ge-GeAr}_3$.

Compound	λ_{max} (Calcd.), nm	Oscillator Strength, <i>f</i>	Transition
$(\text{Me}_3\text{Si})_3\text{Ge-GePh}_3$	228	0.35 (0.15)	HOMO–LUMO+1
$(\text{Me}_3\text{Si})_3\text{Ge-Ge}(\text{C}_6\text{H}_4\text{Me-}p)_3$ (1)	239	0.46 (0.11)	HOMO-2–LUMO
$(\text{Me}_3\text{Si})_3\text{Ge-Ge}(\text{C}_6\text{H}_4\text{OMe-}p)_3$	235	0.57 (0.22)	HOMO-2–LUMO
$(\text{Me}_3\text{Si})_3\text{Ge-Ge}(\text{C}_6\text{H}_4\text{NMe}_2-p)_3$	244	0.28 (0.58)	HOMO-2–LUMO
$(\text{Me}_3\text{Si})_3\text{Ge-Ge}(\text{C}_6\text{H}_4\text{F-}p)_3$ (2)	233	0.28 (0.27)	HOMO-2–LUMO+1
$(\text{Me}_3\text{Si})_3\text{Ge-Ge}(\text{C}_6\text{H}_4\text{CN-}p)_3$	261	0.42 (0.22)	HOMO-2–LUMO+1
$(\text{Me}_3\text{Si})_3\text{Ge-Ge}(\text{C}_6\text{H}_4\text{NO}_2-p)_3$	518	0.18 (0.01)	HOMO-2–LUMO+2

Theoretical analysis of UV/vis absorption spectral data for $(\text{Me}_3\text{Si})_3\text{Ge-GeAr}_3$ (Table 1) shows a good correlation with the experiment (see Table 2 below).

Table 2. Comparison of absorption maxima in UV/visible spectra for 1–3 and related compounds.

Compound	λ_{max} , nm ($\epsilon \times 10^{-4}$, $\text{M}^{-1} \text{cm}^{-1}$)	Solvent	Reference
$\text{Me}_3\text{Ge-Ge}(\text{C}_6\text{H}_4\text{Me-}p)_3$	234 (3.7)	CH_2Cl_2	[27]
$(p\text{-MeC}_6\text{H}_4)_3\text{Ge-Ge}(\text{C}_6\text{H}_4\text{Me-}p)_3$	241 (1.8)	CH_2Cl_2	[42]
$(p\text{-MeC}_6\text{H}_4)_3\text{Ge-Ge}(\text{C}_6\text{F}_5)_3$	234 (4.6)	CH_2Cl_2	[21]
$(p\text{-MeC}_6\text{H}_4)_3\text{Ge-GePh}_3$	240	CH_2Cl_2	[42]
$(\text{Me}_3\text{Si})_3\text{Ge-Ge}(\text{SiMe}_3)_3$	209 (7.8)	<i>n</i> -pentane	[22]
$(\text{Me}_3\text{Si})_3\text{Ge-GeCl}_3$	231 (1.4)	<i>n</i> -hexane	[21]
$(\text{Me}_3\text{Si})_3\text{Ge-GePh}_3$	234 (2.7)	<i>n</i> -hexane	[27]
$\text{Me}_3\text{Si-Ge}(\text{C}_6\text{H}_4\text{Me-}p)_3$	230 (3.3)	<i>n</i> -hexane	[27]
$\text{Me}_3\text{Si-Ge}(\text{C}_6\text{H}_4\text{Me-}p)_3$	231 (1.8)	CH_2Cl_2	[27]
$(t\text{-Bu})\text{Me}_2\text{Si-Ge}(\text{C}_6\text{H}_4\text{Me-}p)_3$	233 (3.2)	<i>n</i> -hexane	[43]
$(t\text{-Bu})\text{Me}_2\text{Si-Ge}(\text{C}_6\text{H}_4\text{Me-}p)_3$	235 (4.5)	CH_2Cl_2	[43]
$[\text{Me}_3\text{Si}]_2\text{-GePh}_2$	238 (1.5)	<i>n</i> -pentane	[44]
$\text{Me}_3\text{Si-Me}_2\text{Si-Ge}(\text{C}_6\text{H}_4\text{Me-}p)_3$	241 (2.5)	CH_2Cl_2	[16]
$(\text{Me}_3\text{Si})_3\text{Ge-Ge}(\text{C}_6\text{H}_4\text{Me-}p)_3$ (1)	239 (3.1)	<i>n</i> -hexane	this work
$(\text{Me}_3\text{Si})_3\text{Ge-Ge}(\text{C}_6\text{H}_4\text{F-}p)_3$ (2)	230 (3.3)	<i>n</i> -hexane	this work
$(\text{Me}_3\text{Si})_3\text{Ge-Ge}(\text{C}_6\text{F}_5)_3$ (3)	242 (3.1)	<i>n</i> -hexane	this work

2.5. UV/Vis Absorption

Absorption data for compounds **1–3** and related derivatives are given in Table 2. In general, investigation of UV/vis absorption is highly important for studies of catenated main group element derivatives and can be regarded as an estimation of conjugation in them.

These data clearly show that in digermanes the absorption maximum (and therefore the HOMO/LUMO gap) depends strongly on σ,π -conjugation (involvement of Ar groups in conjugation with Ge and Ge-Ge frameworks); the presence of aromatic substituents results in a red shift. At the same time, for $(\text{Me}_3\text{Si})_3\text{Ge-GeAr}_3$, the electron properties of Ar affect UV/vis absorption, which is consistent with the DFT data. Thus, compounds with strong acceptor groups are characterized by a greater bathochromic shift; introduction of donating groups also results in red changes in $(\text{C}_6\text{F}_5 > p\text{-MeC}_6\text{H}_4 > \text{Ph} > p\text{-FC}_6\text{H}_4)$ spectra. Furthermore, the Ge-Si conjugation also affects the shift of the absorption band. Besides, linear conjugation is more effective than the branched one (Si-Si-Ge vs. $\text{Si}_3\text{-Ge}$).

3. Materials and Methods

3.1. Experimental Details

All manipulations were performed under a dry and oxygen-free argon atmosphere using the standard Schlenk techniques. The ^1H (400.130 MHz), ^{13}C (100.613 MHz), ^{19}F (376.498 MHz), and ^{29}Si (79.495 MHz) NMR spectra were recorded on a Bruker 400 or Agilent 400MR spectrometer at 298 K. Chemical shifts are given in ppm relative to internal Me_4Si (^1H , ^{13}C , and ^{29}Si NMR spectra) or external CFCl_3 (^{19}F spectra). Elemental analyses were carried out at the Microanalytical Laboratory, Chemistry Department, M.V. Lomonosov Moscow State University, using a Heraeus Vario Elementar instrument or at the Laboratory of Microanalysis, N.D. Zelinsky Institute of Organic Chemistry RAS on a PerkinElmer 2400 Series II CHN Elemental Analyzer. Matrix-assisted laser-desorption/ionization time-of-flight mass spectrometry (MALDI-TOF-MS) analyses were performed on a Microflex (Bruker Daltonics) time-of-flight mass spectrometer; the spectra were recorded in the positive linear mode. UV/visible spectra were obtained using a Thermo Scientific Evolution 300 double-beam spectrophotometer with a 0.10 cm cuvette.

Solvents were dried by standard methods and distilled prior to use. Tetrahydrofuran was stored under solid KOH and then distilled over sodium/benzophenone; *n*-hexane was refluxed and distilled over sodium. CDCl_3 was refluxed and distilled over CaH_2 under argon atmosphere.

Starting materials, $(\text{Me}_3\text{Si})_4\text{Ge}$ [45], $(p\text{-MeC}_6\text{H}_4)_3\text{GeCl}$ [42,46], $(p\text{-FC}_6\text{H}_4)_3\text{GeCl}$ [34], and $(\text{C}_6\text{F}_5)_3\text{GeCl}$ [21], were obtained via previously reported procedures. *t*-BuOK and other reagents were used as supplied (Aldrich).

3.2. X-ray Crystallography

Crystal data, data collection, structure solution and refinement parameters for **1** and **2** are given in Table S1 (Supplementary Materials). Experimental intensities were measured on a Bruker SMART APEX II diffractometer (graphite monochromatized Mo- $K\alpha$ radiation, $\lambda = 0.71073 \text{ \AA}$) using the ω scan mode. The structures were solved by direct methods and refined by full-matrix least-squares on F^2 (SHELXTL) with anisotropic thermal parameters for all non-hydrogen atoms. All hydrogen atoms were placed in calculated positions and refined using a riding model. In **1**, one of the methyl groups was found to be rotationally disordered. X-ray diffraction studies were performed at the Centre of Shared Equipment of IGIC RAS. Crystallographic data were deposited with the Cambridge Crystallographic Data Centre as supplementary publications nos. CCDC-2145489 and 2145490.

3.3. DFT Calculations

The calculations were performed with full geometry optimization and used the GAUSSIAN'09 program package [47]. The absence of imaginary vibration frequencies confirmed the stationary character of the structures. The hybrid *meta* exchange-correlation functional

called M06-2X was used. It is a high-nonlocality functional with double the amount of non-local exchange (2X), parameterized only for nonmetals [48]. We used the time-dependent density functional computations [6–31 G (d, p) basis set], as implemented by Gaussian 09, which were utilized to explore the excited manifold and to compute the possible electronic transitions. The molecular orbitals and UV/visible spectra were constructed using the GaussView program. The UV spectra were calculated in an approximation of the polarizable continuum model in dichloromethane [49].

3.4. Synthesis

Synthesis of $\text{Ar}_3\text{Ge-Ge}(\text{SiMe}_3)_3$. General procedure. Step 1, synthesis of $[(\text{Me}_3\text{Si})_3\text{Ge}^*\text{THF}]$ in situ. The procedure of Marschner et al. was used [30]. Solid *t*-BuOK (0.1540 g, 1.37 mmol) was added to a solution of $(\text{Me}_3\text{Si})_4\text{Ge}$ (0.5000 g, 1.37 mmol) in THF (20 mL). The mixture obtained was stirred for 5 h. The solution of $[(\text{Me}_3\text{Si})_3\text{Ge}^*\text{THF}]$ in THF was used further without additional purification.

Step 2, synthesis of $\text{Ar}_3\text{Ge-Ge}(\text{SiMe}_3)_3$. At -78°C , the solution of $[(\text{Me}_3\text{Si})_3\text{Ge}^*\text{THF}]$ in THF, obtained as stated above in *Step 1*, was added dropwise to a solution of Ar_3GeCl (1.00 eq., 1.37 mmol) in THF (20 mL). The mixture obtained was stirred at the same temperature for 2 h, slowly warmed to room temperature and stirred overnight. Then, all volatile materials were removed under reduced pressure, and the residue was purified by passing through a pad of SiO_2 using petroleum ether as an eluent. After evaporation, the solid obtained was recrystallized from a minimal amount of *n*-hexane to give $\text{Ar}_3\text{Ge-Ge}(\text{SiMe}_3)_3$.

1,1,1-Tris(p-tolyl)-2,2,2-tris(trimethylsilyl) digermane, (p-MeC₆H₄)₃Ge-Ge(SiMe₃)₃ (1). White powder. Yield: 0.6023 g (69%).

¹H NMR (400.130 MHz, CDCl₃): δ 0.14 (s, 27H, 3SiMe₃); 2.34 (s, 9H, 3 MeC₆H₄-p); 7.12 (d, ³J_{H-H} = 7.7 Hz, 6H, 3 *meta*-(*p*-C₆H₄)), 7.33 (d, ³J_{H-H} = 7.7 Hz, 6H, 3 *ortho*-(*p*-C₆H₄)).

¹³C{¹H} NMR (100.613 MHz, CDCl₃): δ 3.30 (¹J_{13C-29Si} = 45.4 Hz, SiMe₃); 21.43 (MeC₆H₄-p); 128.65 (*meta*-C₆H₄), 135.45 (*ortho*-C₆H₄), 136.86 (*ipso*-C₆H₄), 137.76 (*para*-C₆H₄).

²⁹Si{¹H} NMR (79.495 MHz, CDCl₃): δ -4.48 (SiMe₃).

MALDI-TOF MS: *m/z* 638 [M]⁺.

UV/visible absorption (*n*-hexane, λ_{max} in nm (ϵ in M⁻¹ cm⁻¹): 239 (3.1 × 10⁴).

Anal. Calcd for C₃₀H₄₈Ge₂Si₃ (M_w 638.2386): C, 56.46; H, 7.58%. Found: C, 56.22; H, 7.38%.

Single crystals of compound **1** were obtained after recrystallization from *n*-octane at -30°C .

1,1,1-Tris(p-fluorophenyl)-2,2,2-tris(trimethylsilyl) digermane, (p-FC₆H₄)₃Ge-Ge(SiMe₃)₃ (2). White powder. Yield: 0.6226 g (70%).

¹H NMR (400.130 MHz, CDCl₃): δ 0.14 (s, 27H, 3SiMe₃); 7.05 (pt, J_{H-H} = 8.6 Hz, 6H, 3 *meta*-(*p*-C₆H₄)), 7.36 (dd, ³J_{H-H} = 8.4 Hz, ³J_{1H-19F} = 6.3 Hz, 6H, 3 *ortho*-(*p*-C₆H₄)).

¹³C{¹H} NMR (100.613 MHz, CDCl₃): δ 3.24 (¹J_{13C-29Si} = 45.4 Hz, SiMe₃); 115.30 (d, ²J_{13C-19F} = 19.8 Hz, *meta*-C₆H₄), 135.03 (d, ⁴J_{13C-19F} = 3.7 Hz, *ipso*-C₆H₄), 136.95 (d, ³J_{13C-19F} = 7.3 Hz, *ortho*-C₆H₄), 163.38 (d, ¹J_{13C-19F} = 248.1 Hz, *para*-C₆H₄).

¹⁹F NMR (376.498 MHz, CDCl₃): δ -112.83 (1F).

²⁹Si{¹H} NMR (79.495 MHz, CDCl₃): δ -4.30 (SiMe₃).

MALDI-TOF MS: *m/z* 650 [M]⁺.

UV/visible absorption (*n*-hexane, λ_{max} in nm (ϵ in M⁻¹ cm⁻¹): 230 (3.3 × 10⁴).

Anal. Calcd for C₂₇H₃₉F₃Ge₂Si₃ (M_w 650.1303): C, 49.88; H, 6.05%. Found: C, 50.12; H, 5.92%.

Single crystals of compound **2** were obtained after recrystallization from *n*-octane at -30°C .

1,1,1-Tris(p-fluorophenyl)-2,2,2-tris(trimethylsilyl) digermane, (C₆F₅)₃Ge-Ge(SiMe₃)₃ (3). The crude product was purified by column chromatography (SiO₂, petroleum ether, R_f 0.2). White powder. Yield: 0.1124 g (10%).

¹H NMR (400.130 MHz, CDCl₃): δ 0.23 (s, 27H, 3SiMe₃).

$^{13}\text{C}\{^1\text{H}\}$ NMR (100.613 MHz, CDCl_3): δ 3.28 ($^1J_{^{13}\text{C}-^{29}\text{Si}} = 44.3$ Hz, SiMe_3); 135.93–136.35 (m), 138.74–138.85 (m), 142.20–142.59 (m), 146.95–147.13 (m), 145.51–149.56 (m) (C_6F_5). Several signals of carbons of C_6F_5 groups were not found due to low intensity and high value of nuclear coupling.

^{19}F NMR (376.498 MHz, CDCl_3): δ –158.91 – (–158.80) (m, 2F), –147.72 – (–147.33) (m, 1F), –126.49 – (–126.46) (m, 2F).

$^{29}\text{Si}\{^1\text{H}\}$ NMR (79.495 MHz, CDCl_3): δ –5.33 (SiMe_3).

MALDI-TOF MS: m/z 866 $[\text{M}]^+$.

UV/visible absorption (*n*-hexane, λ_{max} in nm (ϵ in $\text{M}^{-1} \text{cm}^{-1}$): 242 (3.1×10^4).

Anal. Calcd for $\text{C}_{27}\text{H}_{27}\text{F}_{15}\text{Ge}_2\text{Si}_3$ (M_w 866.0158): C, 37.45; H, 3.14%. Found: C, 37.08; H, 3.12%.

4. Conclusions

The results reported in the present work can be regarded as significant advances in main group metal chemistry. We showed that arylated and trimethylsilylated oligoorganogermanes could be easily synthesized by the interaction between aryl halogermanes and germyl potassium salts. Effective σ, π -conjugation between different structural fragments, Ar-Ge and Si-Ge-Ge, resulting in a bathochromic shift of absorption bands, was observed; the conjugation was explained by a HOMO/LUMO gap decrease. The conformational behavior of catenated germanes was determined by the steric size of the substituents; the effect of substituents' size on bond lengths was less significant. The influence of chemical (number and type of E atoms in conjugation, electronic effects of substituents) and structural (conformational behavior) factors on the properties of oligogermanes makes them an attractive subject for further investigation by luminescence, conductive, thermal, and electrochemical methods. The intriguing properties of a series of substituted derivatives, found by DFT calculations, especially for a number of electron-withdrawing ($X = \text{NO}_2$) compounds, will stimulate their synthesis.

Supplementary Materials: The following supporting information can be downloaded at: <https://www.mdpi.com/article/10.3390/molecules27072147/s1>, Figures S1–S11 (NMR spectra of the compounds obtained), Figures S12–S14 (UV/vis spectra of the compounds obtained), Table S1 (crystallographic data), Figure S14 (DFT data): Supporting_Information_Molecules.

Author Contributions: Conceptualization, K.V.Z., O.K.P. and A.V.C.; methodology, K.V.Z.; software, K.V.Z., O.K.P. and A.V.C.; validation, K.V.Z., O.K.P. and A.V.C.; formal analysis, K.V.Z.; investigation, K.V.Z., O.K.P. and A.V.C.; resources, K.V.Z.; data curation, K.V.Z.; writing—original draft preparation, K.V.Z.; writing—review and editing, K.V.Z., O.K.P. and A.V.C.; visualization, K.V.Z., O.K.P. and A.V.C.; supervision, K.V.Z.; project administration, K.V.Z.; funding acquisition, K.V.Z., O.K.P. and A.V.C. All authors have read and agreed to the published version of the manuscript.

Funding: This research received no external funding.

Institutional Review Board Statement: Not applicable.

Informed Consent Statement: Not applicable.

Data Availability Statement: Not applicable.

Acknowledgments: Acquiring the NMR spectra was supported in part by the M.V. Lomonosov Moscow State University Program of Development. Single-crystal X-ray diffraction analyses were performed within the State Assignment on Fundamental Research to the N.S. Kurnakov Institute of General and Inorganic Chemistry. We thank the Hochschulrechenzentrum of the Philipps-Universität Marburg for excellent service (DFT calculations).

Conflicts of Interest: The authors declare no conflict of interest. The funders had no role in the design of the study; in the collection, analyses, or interpretation of data; in the writing of the manuscript, or in the decision to publish the results.

Sample Availability: Samples of the compounds are available from the authors.

References

1. Kunkel, C.; Bolte, M.; Lerner, H.-W.; Albert, P.; Wagner, M. Subvalent mixed SixGey oligomers: $(\text{Cl}_3\text{Si})_4\text{Ge}$ and $\text{Cl}_2(\text{Me}_2\text{EtN})\text{SiGe}(\text{SiCl}_3)_2$. *Chem. Commun.* **2021**, *57*, 12028–12031. [[CrossRef](#)] [[PubMed](#)]
2. Binder, M.; Schrenk, C.; Block, T.; Pöttgen, R.; Schnepf, A. $\text{LiGe}(\text{SiMe}_3)_3$: A New Substituent for the Synthesis of Metalloid Tin Clusters from Metastable Sn(I) Halide Solutions. *Molecules* **2018**, *23*, 1022. [[CrossRef](#)]
3. Rivard, E. Group 14 inorganic hydrocarbon analogues. *Chem. Soc. Rev.* **2016**, *45*, 989–1003. [[CrossRef](#)] [[PubMed](#)]
4. Steller, B.G.; Doler, B.; Fischer, R.C. Diaryltin Dihydrides and Aryltin Trihydrides with Intriguing Stability. *Molecules* **2020**, *25*, 1076. [[CrossRef](#)] [[PubMed](#)]
5. Miller, R.D.; Michl, J. Polysilane high polymers. *Chem. Rev.* **1989**, *89*, 1359–1410. [[CrossRef](#)]
6. Amadoruge, M.L.; Weinert, C.S. Singly Bonded Catenated Germanes: Eighty Years of Progress. *Chem. Rev.* **2008**, *108*, 4253–4294. [[CrossRef](#)] [[PubMed](#)]
7. Sita, L.R. Structure/Property Relationships of Polystannanes. In *Advances in Organometallic Chemistry*; Stone, F.G.A., West, R., Eds.; Academic Press: San Diego, CA, USA, 1995; Volume 38, pp. 189–243.
8. Wang, Y.; Quillian, B.; Wei, P.; Yang, X.-J.; Robinson, G.H. New Pb–Pb bonds: Syntheses and molecular structures of hexabiphenyldiplumbane and tri(trisbiphenylplumbyl)plumbate. *Chem. Commun.* **2004**, *19*, 2224–2225. [[CrossRef](#)] [[PubMed](#)]
9. Marschner, C.; Hlina, J. 1.03—Catenated Compounds—Group 14 (Ge, Sn, Pb). In *Comprehensive Inorganic Chemistry II*, 2nd ed.; Reedijk, J., Poeppelmeier, K., Eds.; Elsevier: Amsterdam, The Netherlands, 2013; pp. 83–117.
10. Jovanovic, M.; Michl, J. Alkanes versus Oligosilanes: Conformational Effects on σ -Electron Delocalization. *J. Am. Chem. Soc.* **2022**, *144*, 463–477. [[CrossRef](#)]
11. Léal, M.A.; Begic, K.; Campbell, J.; Kirkman, N.; Myers, D.; Schrick, A.C.; Rheingold, A.L.; Weinert, C.S. Preparation, absorption spectra, and electrochemistry of the trigermanes $\text{R}_3\text{GeGePh}_2\text{GeR}_3$ ($\text{R}_3 = t\text{BuMe}_2$, PhMe_2 , $n\text{Bu}_3$) and tetragermanes $\text{R}_3\text{Ge}(\text{GePh}_2)_2\text{GeR}_3$ ($\text{R}_3 = \text{Et}_3$, $n\text{Bu}_3$). *J. Organomet. Chem.* **2020**, *925*, 121467. [[CrossRef](#)]
12. Foucher, D. Catenated Germanium and Tin Oligomers and Polymers. In *Main Group Strategies towards Functional Hybrid Materials*; Baumgartner, T., Jäkle, F., Eds.; John Wiley & Sons Ltd.: Chichester, UK, 2018; Chapter 9; pp. 209–236.
13. Yu, H.; Ni, C.; Thiessen, A.N.; Li, Z.; Veinot, J.G.C. Synthesis, Properties, and Derivatization of Poly(dihydrogermane): A Germanium-Based Polyethylene Analogue. *ACS Nano* **2021**, *15*, 9368–9378. [[CrossRef](#)]
14. Klausen, R.S.; Ballester-Martínez, E. Organosilicon and Related Group 14 Polymers. In *Reference Module in Chemistry, Molecular Sciences and Chemical Engineering*; Elsevier: Oxford, UK, 2021. [[CrossRef](#)]
15. Su, T.A.; Li, H.; Klausen, R.S.; Kim, N.T.; Neupane, M.; Leighton, J.L.; Steigerwald, M.L.; Venkataraman, L.; Nuckolls, C. Silane and Germane Molecular Electronics. *Acc. Chem. Res.* **2017**, *50*, 1088–1095. [[CrossRef](#)] [[PubMed](#)]
16. Zaitsev, K.V.; Tafeenko, V.A.; Oprunenko, Y.F.; Kharcheva, A.V.; Zhanabil, Z.; Suleimen, Y.; Lam, K.; Zaitsev, V.B.; Zaitseva, A.V.; Zaitseva, G.S.; et al. Molecular Oligogermanes and Related Compounds: Structure, Optical and Semiconductor Properties. *Chem. Asian J.* **2017**, *12*, 1240–1249. [[CrossRef](#)] [[PubMed](#)]
17. Selmani, A.; Schoenebeck, F. Transition-Metal-Free, Formal C–H Gemylation of Arenes and Styrenes via Dibenzothiophenium Salts. *Org. Lett.* **2021**, *23*, 4779–4784. [[CrossRef](#)] [[PubMed](#)]
18. Yu, X.; Lübbesmeyer, M.; Studer, A. Oligosilanes as Silyl Radical Precursors through Oxidative Si–Si Bond Cleavage Using Redox Catalysis. *Angew. Chem. Int. Ed.* **2021**, *60*, 675–679. [[CrossRef](#)] [[PubMed](#)]
19. Samanam, C.R.; Amadoruge, M.L.; Yoder, C.H.; Golen, J.A.; Moore, C.E.; Rheingold, A.L.; Materer, N.F.; Weinert, C.S. Syntheses, Structures, and Electronic Properties of the Branched Oligogermanes $(\text{Ph}_3\text{Ge})_3\text{GeH}$ and $(\text{Ph}_3\text{Ge})_3\text{GeX}$ ($\text{X} = \text{Cl}, \text{Br}, \text{I}$). *Organometallics* **2011**, *30*, 1046–1058. [[CrossRef](#)]
20. Schrick, E.K.; Forget, T.J.; Roewe, K.D.; Schrick, A.C.; Moore, C.E.; Golen, J.A.; Rheingold, A.L.; Materer, N.F.; Weinert, C.S. Substituent Effects in Digermanes: Electrochemical, Theoretical, and Structural Investigations. *Organometallics* **2013**, *32*, 2245–2256. [[CrossRef](#)]
21. Zaitsev, K.V.; Kapranov, A.A.; Churakov, A.V.; Poleshchuk, O.K.; Oprunenko, Y.F.; Tarasevich, B.N.; Zaitseva, G.S.; Karlov, S.S. “Donor–Acceptor” Oligogermanes: Synthesis, Structure, and Electronic Properties. *Organometallics* **2013**, *32*, 6500–6510. [[CrossRef](#)]
22. Baumgartner, J.; Fischer, R.; Fischer, J.; Wallner, A.; Marschner, C.; Flörke, U. Structural Aspects of Trimethylsilylated Branched Group 14 Compounds. *Organometallics* **2005**, *24*, 6450–6457. [[CrossRef](#)]
23. Hlina, J.; Zitz, R.; Wagner, H.; Stella, F.; Baumgartner, J.; Marschner, C. σ -Bond electron delocalization of branched oligogermanes and germanium containing oligosilanes. *Inorg. Chim. Acta* **2014**, *422*, 120–133. [[CrossRef](#)]
24. Wagner, H.; Baumgartner, J.; Müller, T.; Marschner, C. Shuttling Germanium Atoms into Branched Polysilanes. *J. Am. Chem. Soc.* **2009**, *131*, 5022–5023. [[CrossRef](#)]
25. Marschner, C.; Baumgartner, J.; Wallner, A. Structurally and conformationally defined small methyl polysilanes. *Dalton Trans.* **2006**, *48*, 5667–5674. [[CrossRef](#)] [[PubMed](#)]
26. Mallela, S.P.; Geanangel, R.A. Preparation and structural characterization of new derivatives of digermane bearing tris(trimethylsilyl)silyl substituents. *Inorg. Chem.* **1991**, *30*, 1480–1482. [[CrossRef](#)]
27. Zaitsev, K.V.; Lermontova, E.K.; Churakov, A.V.; Tafeenko, V.A.; Tarasevich, B.N.; Poleshchuk, O.K.; Kharcheva, A.V.; Magdesieva, T.V.; Nikitin, O.M.; Zaitseva, G.S.; et al. Compounds of Group 14 Elements with an Element–Element ($\text{E} = \text{Si}, \text{Ge}, \text{Sn}$) Bond: Effect of the Nature of the Element Atom. *Organometallics* **2015**, *34*, 2765–2774. [[CrossRef](#)]

28. Allen, L.C. Electronegativity is the average one-electron energy of the valence-shell electrons in ground-state free atoms. *J. Am. Chem. Soc.* **1989**, *111*, 9003–9014. [[CrossRef](#)]
29. Zaitsev, K.V.; Kharcheva, A.V.; Lam, K.; Zhanabil, Z.; Issabayeva, G.; Oprunenko, Y.F.; Churakov, A.V.; Zaitseva, G.S.; Karlov, S.S. Donor-acceptor molecular oligogermenes: Novel properties and structural aspects. *J. Organomet. Chem.* **2018**, *867*, 228–237. [[CrossRef](#)]
30. Fischer, J.; Baumgartner, J.; Marschner, C. Silylgermylpotassium Compounds. *Organometallics* **2005**, *24*, 1263–1268. [[CrossRef](#)]
31. Hlina, J.; Baumgartner, J.; Marschner, C. Polygermane Building Blocks. *Organometallics* **2010**, *29*, 5289–5295. [[CrossRef](#)]
32. Simon, D.; Häberle, K.; Dräger, M. Über polygermane: XI. Funktionalisierung von hexaphenyldigerman. *J. Organomet. Chem.* **1984**, *267*, 133–142. [[CrossRef](#)]
33. Ng, M.C.C.; Craig, D.J.; Harper, J.B.; van Eijck, L.; Stride, J.A. The Central Atom Size Effect on the Structure of Group 14 Tetratolyls. *Chem. Eur. J.* **2009**, *15*, 6569–6572. [[CrossRef](#)]
34. Zaitsev, K.V.; Lam, K.; Zhanabil, Z.; Suleimen, Y.; Kharcheva, A.V.; Tafeenko, V.A.; Oprunenko, Y.F.; Poleshchuk, O.K.; Lermontova, E.K.; Churakov, A.V. Oligogermenes Containing Only Electron-Withdrawing Substituents: Synthesis and Properties. *Organometallics* **2017**, *36*, 298–309. [[CrossRef](#)]
35. Kurzbach, D.; Yao, S.; Hinderberger, D.; Klinkhammer, K.W. EPR spectroscopic characterization of persistent germlyl-substituted Pb(III)- and Sn(III)-radicals. *Dalton Trans.* **2010**, *39*, 6449–6459. [[CrossRef](#)]
36. Katir, N.; Matioszek, D.; Ladeira, S.; Escudié, J.; Castel, A. Stable *N*-Heterocyclic Carbene Complexes of Hypermetallyl Germanium(II) and Tin(II) Compounds. *Angew. Chem. Int. Ed.* **2011**, *50*, 5352–5355. [[CrossRef](#)] [[PubMed](#)]
37. Nanjo, M.; Sekiguchi, A. Group-14-element-based hybrid dendrimers. Synthesis and characterization of dendrimers with alternating Si and Ge atoms in the chains. *Organometallics* **1998**, *17*, 492–494. [[CrossRef](#)]
38. Yang, L.; Powell, D.R.; Houser, R.P. Structural variation in copper(i) complexes with pyridylmethylamide ligands: Structural analysis with a new four-coordinate geometry index, τ_4 . *Dalton Trans.* **2007**, *9*, 955–964. [[CrossRef](#)]
39. West, R. A new theory for rotational isomeric states: Polysilanes lead the way. *J. Organomet. Chem.* **2003**, *685*, 6–8. [[CrossRef](#)]
40. Laske Cooke, J.A.; Rahbarnoohi, H.; McPhail, A.T.; Wells, R.L.; White, P.S. Reactions of phenylaluminum compounds with $E(\text{SiMe}_3)_3$ ($E = \text{P}$ or As): X-ray crystal structures of $\text{Ph}_3\text{Al}\cdot E(\text{SiMe}_3)_3$ ($E = \text{P}$ or As) and $\text{Ph}_2(\text{Cl})\text{Al}\cdot\text{P}(\text{SiMe}_3)_3$. *Polyhedron* **1996**, *15*, 3033–3044. [[CrossRef](#)]
41. Mallela, S.P.; Saar, Y.; Hill, S.; Geanangel, R.A. Reactions of $\text{LiE}(\text{SiMe}_3)_3$, $E = \text{Si}, \text{Ge}$: X-ray crystal structure of the cyclotetrastannane $[\text{ClSnSi}(\text{SiMe}_3)_3]_4$. *Inorg. Chem.* **1999**, *38*, 2957–2960. [[CrossRef](#)]
42. Amadoruge, M.L.; Short, E.K.; Moore, C.; Rheingold, A.L.; Weinert, C.S. Structural, spectral, and electrochemical investigations of *para*-tolyl-substituted oligogermenes. *J. Organomet. Chem.* **2010**, *695*, 1813–1823. [[CrossRef](#)]
43. Zaitsev, K.V.; Oprunenko, Y.F.; Churakov, A.V.; Zaitseva, G.S.; Karlov, S.S. Reaction of digermenes and related Ge-Si compounds with trifluoromethanesulfonic acid: Synthesis of helpful building blocks for the preparation of Ge-Ge(Si)-catenated compounds. *Main Group Metal Chem.* **2014**, *37*, 67–74. [[CrossRef](#)]
44. Bobbitt, K.L.; Maloney, V.M.; Gaspar, P.P. New photochemical routes to germynes and germenes and kinetic evidence concerning the germylene-diene addition mechanism. *Organometallics* **1991**, *10*, 2772–2777. [[CrossRef](#)]
45. Brook, A.G.; Abdesaken, F.; Söllradl, H. Synthesis of some tris(trimethylsilyl)germyl compounds. *J. Organomet. Chem.* **1986**, *299*, 9–13. [[CrossRef](#)]
46. Lee, V.Y.; Yasuda, H.; Ichinohe, M.; Sekiguchi, A. Heavy cyclopropene analogues R_4SiGe_2 and R_4Ge_3 ($\text{R} = \text{SiMe}_2\text{Bu}_2$)—New members of the cyclic digermenes family. *J. Organomet. Chem.* **2007**, *692*, 10–19. [[CrossRef](#)]
47. Frisch, M.J.; Trucks, G.W.; Schlegel, H.B.; Scuseria, G.E.; Robb, M.A.; Cheeseman, J.R.; Scalmani, G.; Barone, V.; Mennucci, B.; Petersson, G.A.; et al. *Gaussian 09, Revision C.01*; Gaussian Inc.: Wallingford, UK, 2010.
48. Zhao, Y.; Truhlar, D.G. The M06 suite of density functionals for main group thermochemistry, thermochemical kinetics, noncovalent interactions, excited states, and transition elements: Two new functionals and systematic testing of four M06-class functionals and 12 other functionals. *Theor. Chem. Acc.* **2008**, *120*, 215–241.
49. Tomasi, J.; Persico, M. Molecular Interactions in Solution: An Overview of Methods Based on Continuous Distributions of the Solvent. *Chem. Rev.* **1994**, *94*, 2027–2094. [[CrossRef](#)]